Photoinduced formation of gold nanoparticles into vinyl alcohol based polymers

Andrea Pucci,*[ab] Marco Bernabò,[ab] Paolo Elvati,[c] L. Itzel Meza,[d] Fernando Galembeck,[e] Carlos Alberto de Paula Leite,[e] Nicola Tirelli*[f] and Giacomo Ruggeri[ab]

Received 5th August 2005, Accepted 7th October 2005
First published as an Advance Article on the web 11th November 2005
DOI: 10.1039/b511198f

Nanocomposites based on vinyl alcohol-containing polymers and nanostructured gold have been efficiently prepared by a UV photo-reduction process. The very fast process provided dispersed gold nanoparticles with average diameters ranging from 3 to 20 nm depending on the host polymer matrix and the irradiation time. Uniaxial drawing of the irradiated Au/polymer nanocomposites favours the anisotropic distribution of packed assemblies of gold particles, providing oriented films with polarization-dependent tunable optical properties. These pronounced dichroic properties suggest that the nanocomposite films could find potential applications as colour polarizing filters, radiation responsive polymeric objects and smart flexible films in packaging applications.

Introduction

The development of methods to control size, morphology and aggregation of inorganic nanoparticles is a subject of particular interest, since these variables dramatically influence their optical properties, and therefore offer ideal means for controlling them.[1–3] Differently from smooth metal surfaces or metal powders, clusters of noble metals, such as gold, silver or copper, assume a real and natural colour due to the absorption of visible light at the surface plasmon resonance frequency, and this, as described by the Drude–Lorentz–Sommerfeld[1,2] theory and shown by a huge number of experimental data,[2,4] is much affected by cluster size. In particular, the decrease in metal particle size leads to broadening of the absorption band, decrease of the maximum intensity and often to a hypsochromic (blue) shift of the peak, and these effects depend also on cluster topology and packing. For example, the anisotropical orientation of dipoles in nanoparticles by an electric[5,6] or magnetic field,[7,8] or by a templating agent[9–11] or by a uniaxially oriented host polymer matrix,[12–17] generates two different excitation modes: with photons polarized along the aggregation direction, leading to a bathochromic (red) shift of the surface plasmon resonance, or orthogonally to it, resulting in a hypsochromic (blue) shift.[1]

Interestingly, the combination of the optical properties of metal clusters with the mechanical ones of thermoplastic host materials has recently received remarkable attention due to the very attractive optical features of polymer nanocomposites.[12–14,18–23]

When dispersed into polymers in non-aggregated form, nanoparticles with very small diameters (a few nm) allow the preparation of materials with much reduced light scattering properties for applications as optical filters,[14] linear polarizers[12,15,17] and optical sensors.[24] There, the control in nanoparticle size, shape and spatial distribution may actually provide composite material with modulated optical properties.

In the present work, we have used a photochemical, bottom-up approach to prepare gold nanoparticles in a polymer matrix based on vinyl alcohol repeating units, which act as co-reducing agents, as protective agents against particle agglomeration and as macroscopic support. In particular we have compared poly(vinyl alcohol) (PVAl) with two poly(ethylene)-co-(vinyl alcohol) (EVAl) copolymers (with 0.27 and 0.44 ethylene molar fraction), which can reduce well-known drawbacks of PVAl films, *i.e.* low stability at high temperatures and in humid environments.

The direct, photochemical synthesis of gold nanoparticles into the polymer represents an easy, fast and highly competitive method for the preparation of polymeric nanocomposites with tunable and possibly attractive optical properties.

We here discuss the influence of the photochemical process and of the nature of the polymer matrix on the size and aspect of the gold nanoparticles, and how the optical behaviour of these materials may find application in smart packaging.

Experimental

Materials

Hydrogen tetrachloroaurate(III) trihydrate ($HAuCl_4$, 99.9+%) and all the other chemicals were purchased from Aldrich and were used without further purification.

[a]*Department of Chemistry and Industrial Chemistry, University of Pisa, Via Risorgimento 35, 56126, Pisa, Italy. E-mail: apucci@dcci.unipi.it*
[b]*INSTM, Pisa Research Unit, Via Risorgimento 35, 56126, Pisa, Italy. E-mail: apucci@dcci.unipi.it*
[c]*Scuola Normale Superiore, Piazza dei Cavalieri 7, 56126, Pisa, Italy*
[d]*Centre for Microporous Materials, School of Chemistry, University of Manchester, P.O. Box 88, Sackville Street, Manchester, M60 1QD, United Kingdom*
[e]*Institute of Chemistry, Universidade Estadual de Campinas, P.O. Box 6154, CEP 13084-862, SP, Brazil*
[f]*School of Pharmacy and Molecular Materials Centre, University of Manchester, Coupland III, Coupland Street/Oxford Road, Manchester, M13 9PL, United Kingdom. E-mail: nicola.tirelli@manchester.ac.uk*

Sample nomenclature

Three polymer matrices were used:

Poly(vinyl alcohol) (PVAl, 99+% hydrolyzed, $\bar{M}_w$ = 146 000–186 000 supplied by Aldrich).

Poly(ethylene)-co-(vinyl alcohol) with 27% by mol of ethylene content ($EVAl_{27}$, $\leqslant$0.7% of polymerized vinyl acetate, melt index (210 °C, ASTM D 1238) = 3.90 g 10 min^{-1}, density (25 °C) = 1.2 g mL^{-1}, supplied by Aldrich).

Poly(ethylene)-co-(vinyl alcohol) with 44% by mol of ethylene content ($EVAl_{44}$, $\leqslant$0.7% of polymerized vinyl acetate, melt index (210 °C, ASTM D 1238) = 3.5 g 10 min^{-1}, density (25 °C) = 1.14 g mL^{-1}, supplied by Aldrich).

Samples were named by listing metal, polymer and irradiation time, *e.g.* Au/$EVAl_{27}$ 5 min.

Nanocomposite preparation

The typical procedure for the preparation of gold/polymer nanocomposites is reported as follows:

0.335 g of the polymer (PVAl or EVAl) was dissolved in 20 mL of solvent (respectively deionised water for PVAl, dimethylsulfoxide for EVAl matrices) under stirring at 110 °C. After cooling to room temperature, 100 mg of ethylene glycol (30 wt%) and 13.4 mg of $HAuCl_4$ (4 wt%) were added to the solution. The resultant yellow solution was cast into a polytetrafluoroethylene (PTFE) Petri dish and kept in the dark during solvent evaporation (2 days under a hood at room temperature for PVAl and at 45 °C for EVAl solutions) to prevent photo-reduction. The dried film (thickness ~60–80 μm) was recovered and irradiated at a distance of 25 cm with a 400 W high pressure mercury lamp (Polymer 400 Helios Italquarz, 5950 and 9450 μW cm^{-2} at 254 and 365 nm, respectively) for different times.

Oriented composites were obtained by uniaxial tensile drawing of the polymer matrix on a thermostatically controlled hot stage at 110 °C for PVAl mixtures and 90 °C for EVAl films. The draw ratio, defined as the ratio between the final and the initial length of the sample respectively, was determined by measuring the displacement of ink-marks printed onto the films before stretching.

Physico-chemical characterization

Attenuated total reflectance Fourier transform infrared (ATR/FTIR) spectra were recorded on polymer films with the help of a Perkin-Elmer Spectrum One spectrometer fitted with Universal ATR (UATR, DiComp™ crystal) accessories. Differential scanning calorimetry (DSC) analyses were performed under nitrogen flux (80 mL min^{-1}) with a Mettler-Toledo/DSC 822^e equipped with a cooling system. The calibration was performed with zinc and indium. Heating and cooling thermograms were carried out at a standard rate of 20 °C min^{-1}. Bright field transmission electron microscopy (TEM) pictures were obtained on polymer composites by using a Carl Zeiss CEM-902 transmission electron microscope, equipped with a Castaing–Henry–Ottensmeyer energy filter spectrometer within the column. Other experimental details regarding TEM and sample preparation are presented elsewhere.[12] Particle analysis was performed using the public domain Image Tool 3.00 version image analyzer program developed at the University of Texas Health Science Center in San Antonio and available on Internet at http://ddsdx.uthscsa.edu/dig/itdesc.html.

X-Ray diffraction (XRD) patterns were obtained in Bragg–Brentano geometry with a Siemens D500 KRISTALLOFLEX 810 (CT: 1.0 s; SS: 0.050 dg and Cu Kα, λ = 1.541 Å) diffractometer. Data were acquired at room temperature.

Deionised water static contact angle measurements on polymer films were made using the sessile drop method with a CAM 200 instrument (KSV Instruments Ltd, Finland), which utilises a digital CCD camera with telecentric zoom optics and subsequent drop shape analysis using the Young–Laplace method. A minimum of four measurements were made on the same specimen.

Atomic force microscopy (AFM) images were recorded on a Nanoscope III Multimode microscope operating in Contact Mode using a silicon nitride tip with a force constant of 0.32 Nm^{-1}. Optical microscopy images were obtained with the help of a Reichert Polyvar optical microscope equipped with crossed polarizers. UV–vis absorption spectra of polymer films were recorded under isotropic conditions with a Perkin-Elmer Lambda 650, and in linearly polarized light by mounting motor-driven Glan–Taylor linear polarizers. The film roughness was diminished using ultra-pure silicon oil (poly(methylphenylsiloxane), 710® fluid, Aldrich) to reduce surface scattering between the polymeric films and the quartz slides used to keep them planar.

Origin 7.5, software by Microcal Origin®, was used in the analysis of the XRD and absorption data.

Results and discussion

Preparation of gold/PVAl nanocomposites

Gold nanoparticles were prepared within a poly(vinyl alcohol) (PVAl) polymer matrix by a photochemical method as described in literature.[25–27] PVAl and the hydrogen tetrachloroaurate(III) hydrate ($HAuCl_4$, the Au(III) precursor, 4 wt%) were dissolved in deionised water with the addition of some (30 wt%) ethylene glycol (EG), casted in a film and then irradiated for different times with a 400 W high pressure Hg UV lamp, to promote the reduction of the Au(III) precursor and the formation of Au(0) clusters. The resulting gold particles were efficiently stabilized by the presence of electron-donor hydroxyl groups in the PVAl matrix, which prevented agglomeration and formation of micro-sized phase separated metal aggregates.

Before irradiation the film has a light yellow colour, as a result of the absorption at about 300 nm of the Au^{3+} ions (owing to the ligand-to-metal charge transfer (LMCT)[28]) dissolved in the PVAl matrix, and turns purple after just five minutes of irradiation, due to the presence of the surface plasmon absorption band at about 550 nm (Fig. 1).

The 300 nm absorption band almost disappears just after 5–10 minutes of irradiation indicating that the Au^{3+} ions are quickly converted to nanostructured Au(0) even in a solid host matrix. The different absorption features (band width, intensity and ~12 nm shift of the peak) at 5 and 10 minutes of irradiation may be caused by an increase in the number of

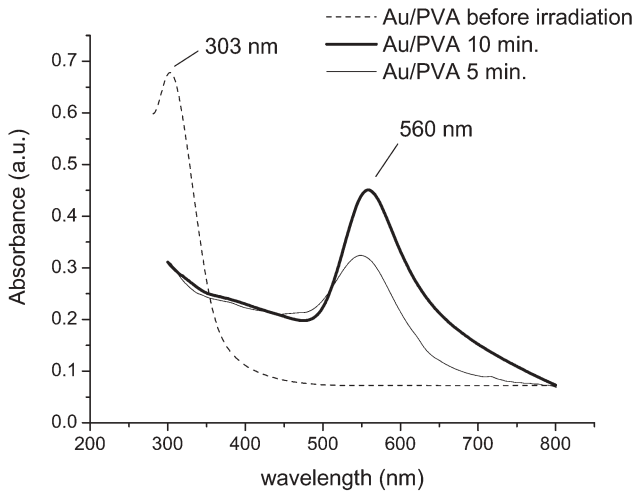

Fig. 1 UV–vis absorption spectra of Au/PVAl film before and after UV irradiation.

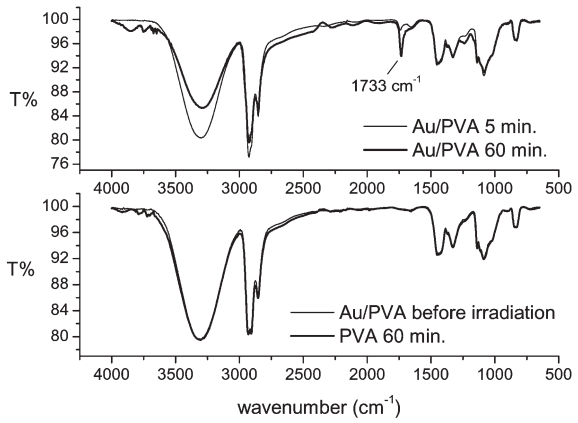

Fig. 2 ATR/FTIR spectra of Au/PVAl film before and after UV irradiation and neat PVAl film irradiated for 60 min.

nanoparticles with irradiation time, although differences in particle size and shape cannot be ruled out, as in other literature reports.[2,27,29]

Literature reports describe the photo-reduction as a stepwise mechanism: the UV radiation initially converts $AuCl_4^-$ to $AuCl_3^-$ through excitation in the LMCT (ligand-to-metal charge transfer) band. After an induction period, $AuCl_3^-$ is progressively converted to $AuCl_2^-$ and finally to Au(0), which self-assembles in nanostructured gold clusters.[25,30] Photoinitiators have been used for accelerating the formation of the clusters, and this has also been shown to provide much more homogeneous nanocomposite films.[31,32]

Alcohols with available α hydrogen atoms have also been used as additives for more efficient photo-reduction reactions,[27,33] following a completely different reaction mechanism, as shown in Scheme 1.

In our case, the use of alcohols (above all ethylene glycol) resulted in the absence of any prolonged induction period, since the surface plasmon resonance occurs after just 5 minutes of irradiation. More importantly, after photo-reduction the samples showed IR absorptions typical of aldehyde groups in the carbonyl region at about 1740–1720 cm^{-1} (Fig. 2).[34] These bands are absent in a matrix of pure PVAl, even after photoirradiation, and in the Au/PVAl film before irradiation, and can therefore be associated with alcohol-mediated photo-reduction, which proves the mechanism shown in Scheme 1.

Bright-field TEM images of Au/PVAl films irradiated for 5 minutes (Au/PVAl 5 min) evidenced the formation of nanoparticles with approximately spherical shapes (Fig. 3a), a mean size of 12 ± 6 nm and quite a broad monomodal distribution (Fig. 3b). Electron diffraction analysis confirmed that these particles were composed of Au(0).

XRD analysis (Fig. 4) has shown that, although the system only partly showed the diffuse broad contribution of the

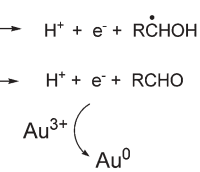

Scheme 1 Photo-reduction mechanism of Au(III) ions promoted by primary alcohols.

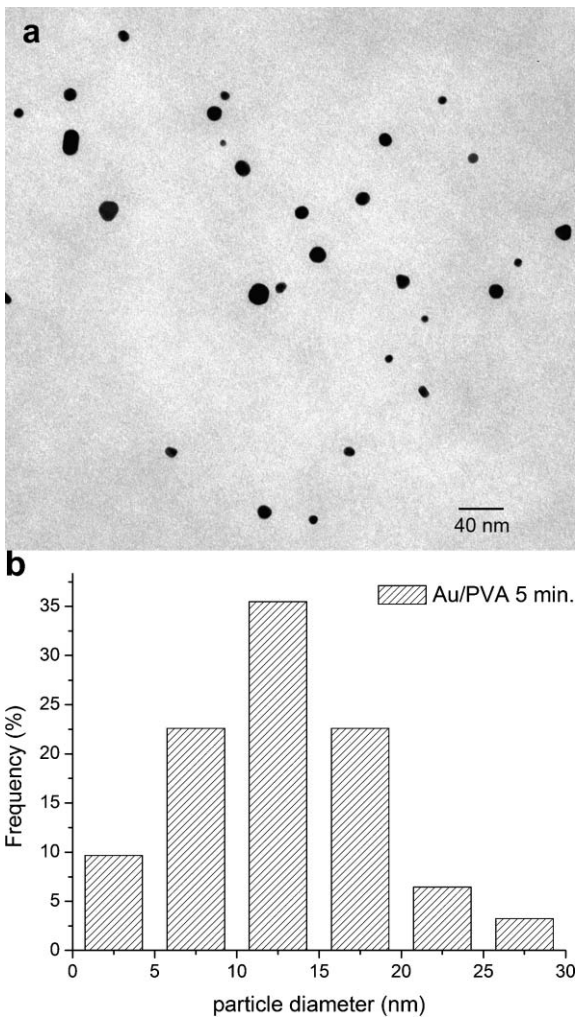

Fig. 3 Bright-field transmission electron micrograph (a) and particle size distribution (b) of Au/PVAl film irradiated for 5 min.

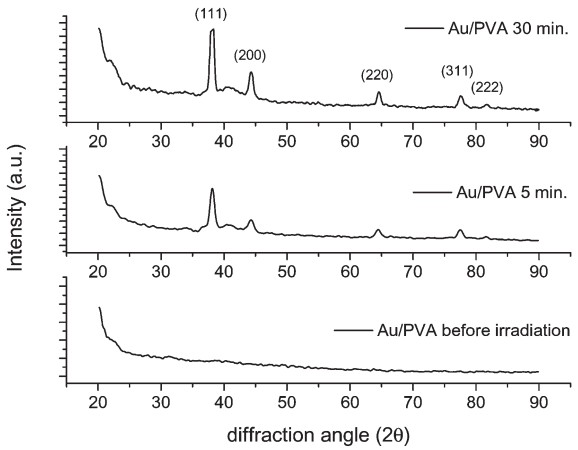

Fig. 4 X-Ray diffraction patterns of Au/PVAl films before and after UV irradiation for 5 and 30 min respectively.

semi-crystalline PVAl matrix centred at about $2\theta = 20^{\circ}$, corresponding to the (101) plane of PVAl crystals, before irradiation ,[35] new diffraction peaks appeared after just 5 minutes of UV illumination which can be assigned to the face-centred cubic (fcc) unit cell of gold.[36] With increasing irradiation time, the signal to noise ratio of the Au peaks improves indicating the progressive formation of nanostructured metallic Au(0) during the photo-reduction process. Application of Scherrer's equation[37] $0.9\lambda/\Delta(2\theta)\cos\theta$ to the Au(111) peak of the Au/PVAl 5 min XRD pattern suggests a mean crystallite size of approximately 12 nm which agrees well with the TEM measurements.

A longer irradiation time (30 min) apparently caused a sound increase in the number of gold nanoparticles (Fig. 5a). In addition, the prolonged irradiation seemed to promote the generation of a large number of smaller gold nanoparticles, lowering their average particle size down to 5 ± 3 nm (Fig. 5b). This phenomenon is likely caused by the fact that, due to the decreased concentration of Au, the nucleation rate became more and more competitive with the growth rate. Further UV exposure, up to 2 hours, seemed merely to promote some agglomeration of the previously formed gold particles by the coalescence phenomenon[2] leading to Au/PVAl nanocomposites with an average size of dispersed gold colloids of about 10 ± 5 nm. This phenomenon may happen during irradiation without being related to photo-reduction reactions; the very high density of the UV radiation energy may heat the film surface to up to 60 °C, close to the PVAl glass transition temperature. We hypothesize that this can favour agglomeration and coalescence phenomena, which can take place on a much quicker timescale on heating than at room temperature.

Preparation of gold/EVAl nanocomposites

Poly(ethylene)-co-(vinyl alcohol) (EVAl) containing different amounts of apolar and in principle more stable ethylene units (27 and 44% by mol, respectively) have been used as an alternative host matrix.

The nanocomposite preparation was substantially analogous to that of PVAl-containing samples, except for the use of

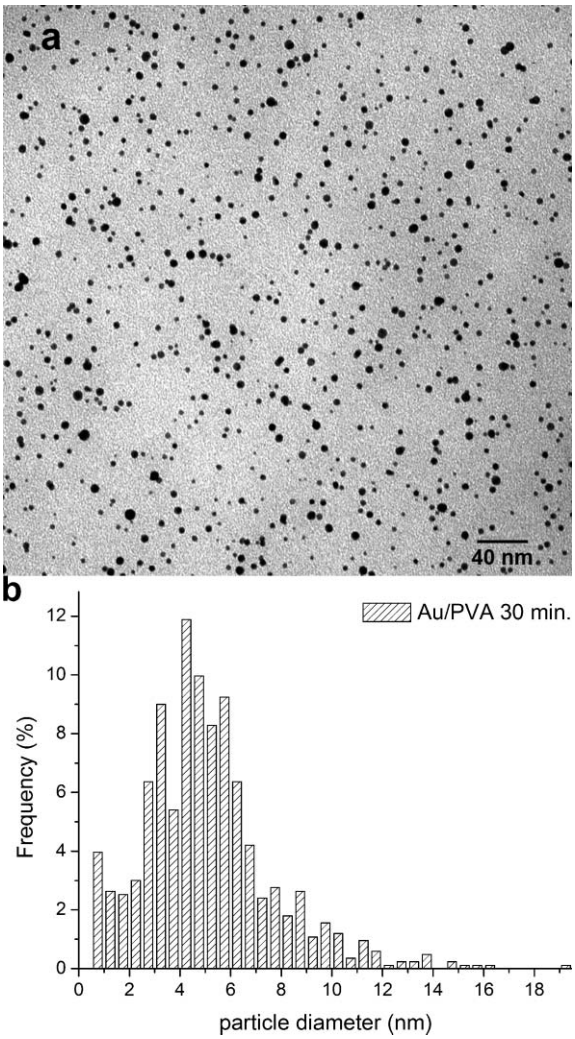

Fig. 5 Bright-field transmission electron micrograph (a) and particle size distribution (b) of Au/PVAl film irradiated for 30 min.

dimethylsulfoxide (DMSO) as a solvent, since EVAl is insoluble in water. Analogous to Au/PVAl composites, the colour changed from pale yellow to homogeneously purple upon irradiation; however, as expected from the lower –OH content of the copolymers and hence the reduced possibility of stabilizing the colloidal interface, the photo-reduction produced larger Au(0) colloids. This was particularly evident at the early stages of the process: after 5 minutes ($Au/EVAl_{27}$ 5 min) an average particle size of about 23 ± 12 nm was recorded, well above the value of 12 ± 6 nm reported for the similar Au/PVAl 5 min (Fig. 6).

As for PVAl-containing nanocomposites, the average particle size decreased with increasing irradiation time, from 23 ± 12 nm at 5 min to 4 ± 3 nm at 30 min, due to the formation of a large number of very small gold nanoparticles with $\text{Ø} \sim 2$–3 nm (Fig. 7).

Interestingly, TEM measurements of the cross-section of the $Au/EVAl_{27}$ 30 min film showed that most smaller particles are located in the inner part of the film (regions B and C), while the area close to the irradiated surface (A) has the highest density of larger particles (Fig. 8).

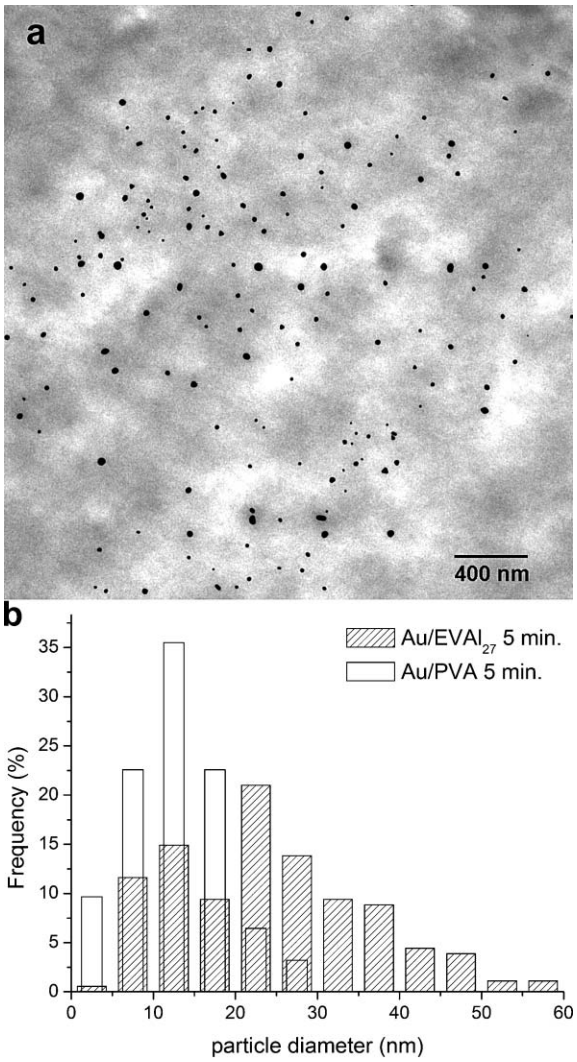

Fig. 6 Bright-field transmission electron micrograph (a) and particle size distribution (b) of Au/EVAl$_{27}$ and Au/PVAl films irradiated for 5 min.

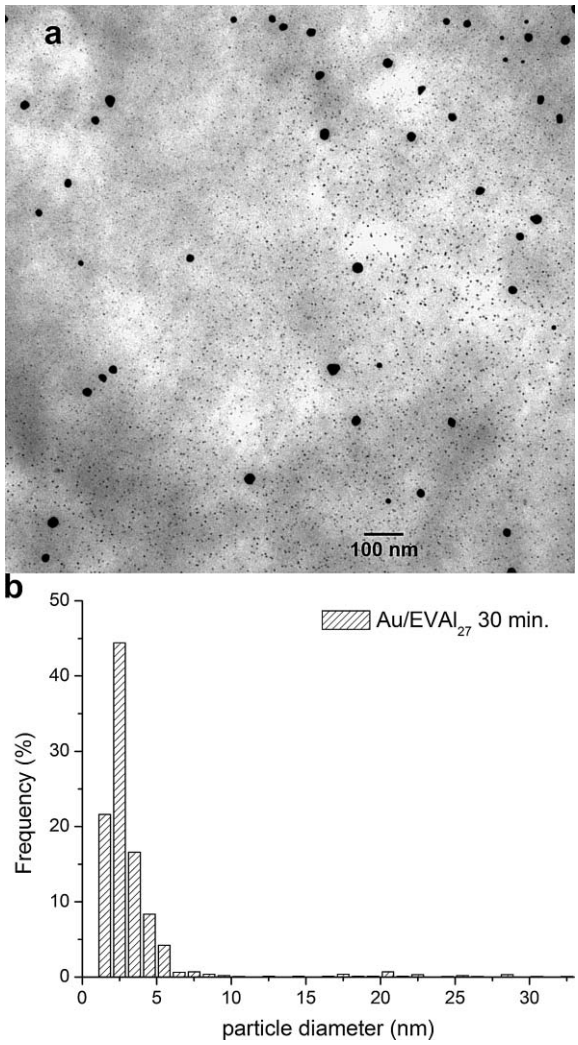

Fig. 7 Bright-field transmission electron micrograph (a) and particle size distribution (b) of Au/EVAl$_{27}$ film irradiated for 30 min.

More precisely, in area A, which was nearest to the UV source, particles with a size of 15–20 nm are a major component of the total particle count. However, they are fewer in number in the other areas, so much so as to be virtually absent in region C, where only a monomodal size distribution centred at about 2–3 nm was recorded.

Also in Au/PVAl nanocomposites smaller particles were generated at longer irradiation times, but with smaller differences between larger and smaller particles and above all with apparently no differences along the film section. The heterogeneity along the film thickness therefore cannot be ascribed to *e.g.* a reduction in the UV energy density, which should cause the same effect in PVAl.

We have, on the contrary, identified two possible effects, which, in combination, may explain the different morphologies observed:

(1) due to the lower surface energy of ethylene units, the polymer close to the air-exposed surface has a lower alcohol content; this increase in surface hydrophobicity is apparent from a quick analysis of the pure polymer–water contact angles: 75 $\pm$ 4° for PVAl, 96 $\pm$ 4° for EVAl$_{27}$, 101 $\pm$ 1° for EVAl$_{44}$. Most likely, it has also a low glass transition temperature (which is already markedly lower than PVAl; PVAl: T_g = 79 °C, EVAl$_{27}$: T_g = 62 °C, EVAl$_{44}$: T_g = 49 °C). As a result, smaller nanoparticles are less stabilized and can easily coalesce to yield bigger aggregates;

(2) as a consequence of the formation of this "hydrophobic skin" and of the use of a less volatile solvent (DMSO *vs.* water), we expect that the inner part of the film is likely to retain more ethylene glycol than in the case of PVAl, and more DMSO too, which could also be a good ligand, with a higher possibility of stabilizing small nanoparticles. This is particularly true for the regions richer in vinyl alcohol, where ethylene glycol and DMSO are more soluble.

A simple consequence of these hypotheses would be the complete absence of nanoparticles from the film surface in Au/EVAl nanocomposites, where hydroxyl groups are supposed to be absent, and their presence in the film surface of Au/PVAl.

This situation was indeed proven by a surface study using atomic force microscopy (AFM). Both non-oriented (data not reported) and oriented films were investigated; the oriented

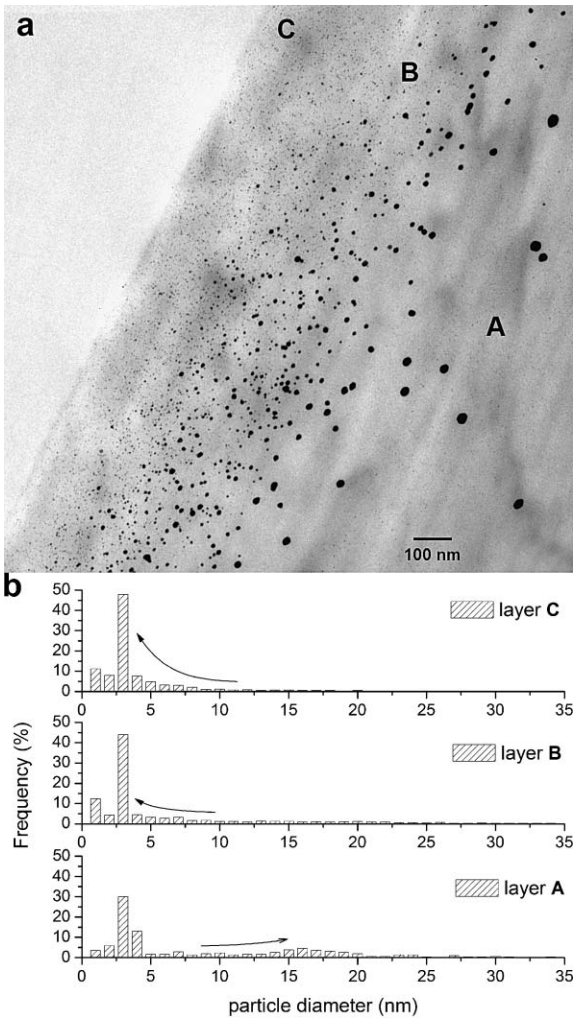

Fig. 8 Bright-field transmission electron micrograph (a) of the cross-section of Au/EVAl$_{27}$ film irradiated for 30 min and particle size distribution (b) for the A, B and C internal layers.

films were uniaxially stretched at respectively 110 °C for PVAl and at 90 °C for EVAl at a drawing ratio (Dr, defined as the ratio between the final and the initial length of the samples) of between 5 and 6, in order to obtain materials with interesting anisotropic optical properties (see below, ''Optical properties''). AFM images of Au/EVAl nanocomposites showed only the corrugate surface of the films and the oriented texture induced by the alignment of the macromolecular chains along the stretching direction (Dr = 6, Fig. 9).

In contrast, the Au/PVAl oriented films (Dr = 5) clearly displayed gold nanoparticles exposed on the polymer surface (Fig. 10).

In particular, the height analysis and the surface plot evidenced particles with an average size of more than 30 nm, predominantly distributed along the drawing direction.

We therefore hypothesize the differences in PVAl nanocomposites to be rationalized as: (1) ethylene-rich regions—there is a more polarized size distribution, due to the lower coordinating power of the matrix, but the mechanism and the time evolution of the nanoparticle formation follow the same time line as for PVAl; (2) inner or alcohol-rich regions—the

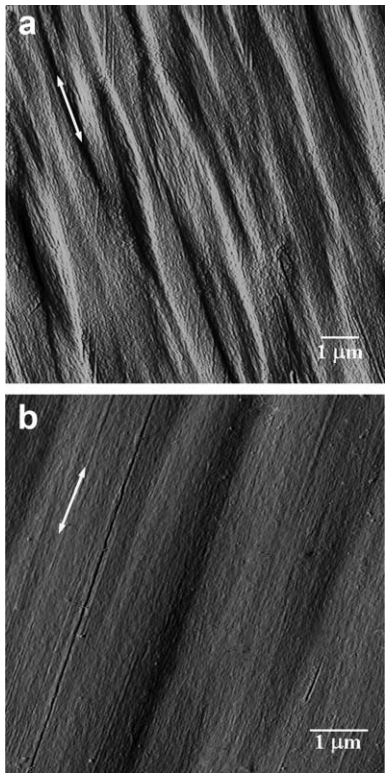

Fig. 9 8 × 8 μm^2 AFM deflection images of oriented Au/EVAl$_{27}$ (a) and Au/EVAl$_{44}$ (b) both irradiated for 30 min. The white arrows denote the drawing direction of the films.

formation of larger aggregates is hindered by the permanence of solvent/reactants, the smaller nanoparticles are formed (according to the same kinetics as in (1) or even faster), due to the presence of a possibly higher concentration of ethylene glycol.

More detailed investigations are currently ongoing, with the aim of revealing how different evaporation methods can influence the spatial homogeneity of size distribution and of quantitatively relating the concentrations of DMSO and ethylene glycol to the particle dimensions.

Finally, as in Au/PVAl nanocomposites, UV irradiation for up to 120 minutes promoted a slight increase in nanoparticle dimensions, from 4 ± 3 to 6 ± 3, which we again ascribed to coalescence during the prolonged UV illumination.

Optical properties of oriented Au/polymer nanocomposites

It has been reported that the uniaxial tensile drawing of Au/polymer composite films can efficiently promote the anisotropic packing of embedded gold nanoparticles.[12,14,17]

Anisotropically distributed and interacting gold particles are known to show a bathochromically (*i.e.* red) shifted absorption band, when the polarization vector of the photons is aligned with the stretching direction of the film, and a hypsochromic (blue) shift for cross-polarized absorption.[2,14] Accordingly, in our case, the oriented Au/polymer nanocomposite films based on both PVAl and EVAl matrices displayed an absorption behaviour strongly dependent on the polarization direction of the incident light (Fig. 11).

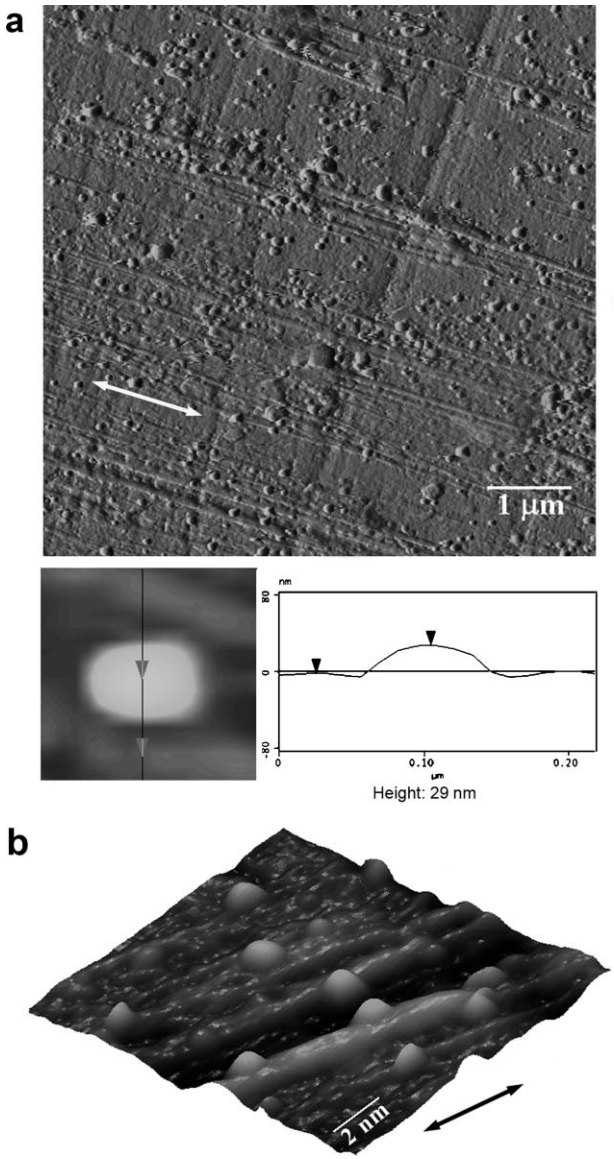

Fig. 10 $8 \times 8\ \mu m^2$ AFM deflection image of oriented Au/PVAl film irradiated for 30 min and cross-sectional analysis of the same film (a). Surface plot of the same AFM image (b). The arrows denote the drawing direction of the films.

The presence of a clear isosbestic point (inset of Fig. 11) centred at about 540 nm may suggest the existence of different populations of absorbing particles, whose spectra are those recorded at the polarizing angles (φ) of 0° and 90°, respectively. The shifts in wavelength and in absorbance between the absorption at 0° and 90° ($\Delta\lambda$ and ΔA, respectively) are reported in Table 1.

Almost all Au/polymer oriented composites showed high dichroism, with $\Delta\lambda$ peaks even higher than 40 nm for films irradiated for just 5–15 minutes. Apparently, the smaller gold particles (Ø $\leqslant$ 3–4 nm, according to TEM measurements) generated upon prolonged irradiation are scarcely sensitive to the matrix anisotropic orientation, as similarly reported for small gold particles (Ø $\sim$ 3–4 nm) embedded into ultra high molecular weight polyethylene composites.[12] This leads to an absorption behaviour which is not very sensitive to the

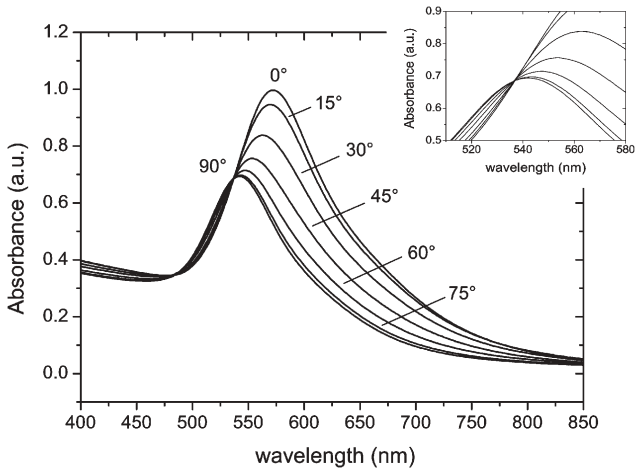

Fig. 11 UV–vis spectra of Au/EVAl$_{27}$ 30 min. oriented film (Dr = 6) as a function of the angle (φ) between the polarization of the light and the drawing direction of the film, and enlargement of the isosbestic point visible region (inset).

Table 1 Dichroic optical performances of oriented Au/polymer nanocomposites

Sample	Dr	$\Delta\lambda$ (nm)	ΔA (a.u.)
Au/PVAl 5 min	5	83	0.71
Au/PVAl 15 min	5	38	0.49
Au/PVAl 30 min	5	26	0.39
Au/PVAl 60 min	4	16	0.18
Au/EVAl$_{27}$ 5 min	6	45	0.20
Au/EVAl$_{27}$ 15 min	6	30	0.19
Au/EVAl$_{27}$ 30 min	6	29	0.27
Au/EVAl$_{27}$ 60 min	5	9	0.11
Au/EVAl$_{44}$ 5 min	5	70	0.53
Au/EVAl$_{44}$ 15 min	6	42	0.20
Au/EVAl$_{44}$ 30 min	6	19	0.15
Au/EVAl$_{44}$ 60 min	5	9	0.10

polarization direction of the incident light, and thus to composite films with low $\Delta\lambda$ values. As evidenced by Fig. 12 for oriented Au/PVAl 30 min. (Dr = 5), the larger particles (Ø $\sim$ 7–8 nm) which were possibly created during the initial stage of photo-reduction and located near the film surface, end up well packed along the drawing direction and grouped in very close assemblies, whereas a number of smaller particles are isotropically distributed within the film.

The dichroic behaviour of oriented Au/polymer composites is even better evidenced by optical microscopy in polarized light (Fig. 13): the surface plasmon resonance shift from $\varphi = 0°$ (parallel to the drawing direction) to $\varphi = 90°$ (perpendicular) is associated with a clear change in colour from blue to purple.

Conclusions

In summary, we have efficiently prepared, by a photo-reduction mechanism, polymer composites containing nano-structured gold particles, starting with a $HAu^{III}Cl_4$ gold precursor dissolved in different vinyl alcohol-containing polymer matrices.

The UV illumination initially generated gold nanoparticles with an average diameter ranging from 12–23 nm, depending

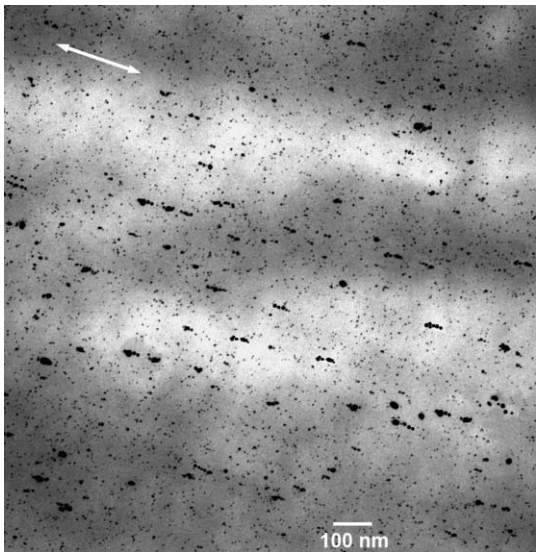

Fig. 12 Bright-field transmission electron micrograph of Au/PVAl 30 min oriented film (Dr = 5). The white arrow denotes the drawing direction of the films.

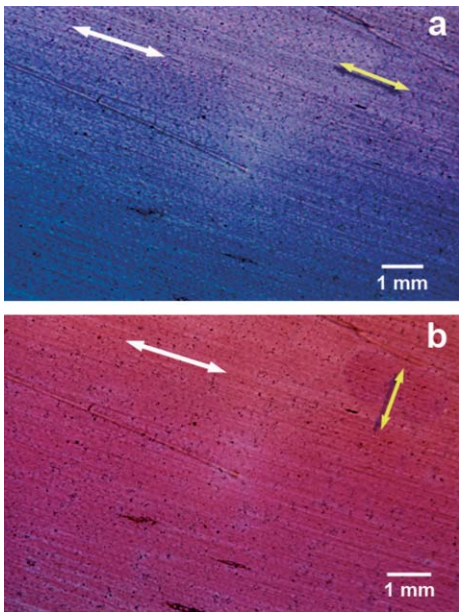

Fig. 13 Optical microscopy images of oriented Au/EVAl$_{44}$ oriented film (Dr = 5) with polarization direction of the incident light parallel (a) and perpendicular (b) to the drawing direction. The white arrows denote the stretching direction of the film, whereas the yellow ones indicate the direction of the electric vector of polarized light.

on the nature of the polymeric film. Longer irradiation times produced a very large number of smaller particles (Ø ~3–4 nm). Uniaxial drawing of the Au/polymer composites promoted anisotropic packing of the embedded gold nanoparticles (particularly the large ones) along the stretching direction of the film, resulting in a shift of the surface plasmon resonance of gold well above 30–40 nm (83 nm max.) and thus producing a well-defined polarization-dependent colour change from blue to purple.

These results are similar to those previously reported for optically anisotropic polyethylene/gold nanocomposites obtained by introducing preformed and annealed alkyl–thiol-protected gold nanoparticles in high-density polyethylene.[17] However, the UV photo-generation of gold nanoparticles directly onto an Au(III)/polymer film precursor, the method reported in this work, represents an innovative, easier, faster and very competitive technique for the preparation of these polymeric nanocomposites for potential applications as colour polarizing filters, radiation responsive polymeric objects and as smart and intelligent flexible films in packaging applications.

Acknowledgements

The authors wish to express their thanks to Prof. Francesco Ciardelli (DCCI, Pisa) for the very helpful discussions and Prof. Michael W. Anderson (Centre for Microporous Materials, University of Manchester, UK) for the use of the AFM. Financial support by MIUR-FIRB 2003 D.D.2186 grant RBNE03R78E is kindly acknowledged. FG acknowledges support from the CNPq/PADCT/Millenium Institutes Program.

References

1 K. J. Klabunde, *Nanoscale Materials in Chemistry*, Wiley Interscience, New York, 2001.
2 U. Kreibig and M. Vollmer, *Optical Properties of Metal Clusters (Springer Series in Materials Science 25)*, Springer–Verlag, Berlin, 1995.
3 K. L. Kelly, E. Coronado, L. L. Zhao and C. Schatz George, *J. Phys. Chem. B*, 2003, **107**, 668–677.
4 M.-C. Daniel and D. Astruc, *Chem. Rev.*, 2004, **104**, 293–346.
5 A. Abdolvand, A. Podlipenski, G. Seifert, H. Graener, O. Deparis and P. G. Kazansky, *Opt. Express*, 2005, **13**, 1266–1274.
6 J. Muller, C. Sonnichsen, H. von Poschinger, G. von Plessen and T. A. Klar, *Appl. Phys. Lett.*, 2002, **81**, 171–173.
7 P. Crespo, R. Litran, T. C. Rojas, M. Multigner, J. M. de la Fuente, J. C. Sanchez-Lopez, M. A. Garcia, A. Hernando, S. Penades and A. Fernandez, *Phys. Rev. Lett.*, 2004, **93**, 087204.
8 V. V. Krishnamurthy, A. S. Bhandar, M. Piao, I. Zoto, A. M. Lane, D. E. Nikles, J. M. Wiest, G. J. Mankey, L. Porcar and C. J. Glinka, *Phys. Rev. E: Stat. Phys., Plasmas, Fluids, Relat. Interdiscip. Top.*, 2003, **67**, 051406.
9 N. A. F. Al-Rawashdeh, M. L. Sandrock, C. J. Seugling and C. A. Foss Jr., *J. Phys. Chem. B*, 1998, **102**, 361–371.
10 M. Brust and C. J. Kiely, *Colloids Surf., A*, 2002, **202**, 175–186.
11 Y. Lin, A. Boeker, J. He, K. Sill, H. Xiang, C. Abetz, X. Li, J. Wang, T. Emrick, S. Long, Q. Wang, A. Balazs and T. P. Russell, *Nature*, 2005, **434**, 55–59.
12 A. Pucci, N. Tirelli, E. A. Willneff, S. L. M. Schroeder, F. Galembeck and G. Ruggeri, *J. Mater. Chem.*, 2004, **14**, 3495–3502.
13 A. Pucci, P. Elvati, G. Ruggeri, V. Liuzzo, N. Tirelli, M. Isola and F. Ciardelli, *Macromol. Symp.*, 2003, **204**, 59–70.
14 W. Caseri, *Macromol. Rapid Commun.*, 2000, **21**, 705–722.
15 Y. Dirix, C. Bastiaansen, W. Caseri and P. Smith, *Adv. Mater.*, 1999, **11**, 223–227.
16 Y. Dirix, C. Bastiaansen, W. Caseri and P. Smith, *J. Mater. Sci.*, 1999, **34**, 3859–3866.
17 Y. Dirix, C. Darribere, W. Heffels, C. Bastiaansen, W. Caseri and P. Smith, *Appl. Opt.*, 1999, **38**, 6581–6586.
18 A. Heilmann, *Polymer Films with Embedded Metal Nanoparticles*, Springer, Berlin, 2003.
19 L. L. Beecroft and C. K. Ober, *Chem. Mater.*, 1997, **9**, 1302–1317.
20 R. J. Gehr and R. W. Boyd, *Chem. Mater.*, 1996, **8**, 1807–1819.
21 G. Carotenuto and L. Nicolais, *J. Mater. Chem.*, 2003, **13**, 1038–1041.

22 R. Salvati, A. Longo, G. Carotenuto, S. De Nicola, G. P. Pepe, L. Nicolais and A. Barone, *Appl. Surf. Sci.*, 2005, **248**, 28–31.
23 L. Nicolais and G. Carotenuto, *Metal–Polymer Nanocomposites*, John Wiley & Sons, Inc., New York, 2005.
24 S. Enoch, R. Quidant and G. Badenes, *Opt. Express*, 2004, **12**, 3422–3427.
25 S. Dong, C. Tang, H. Zhou and H. Zhao, *Gold Bull.*, 2004, **37**, 187–195.
26 Y. Zhou, C. Y. Wang, Y. R. Zhu and Z. Y. Chen, *Chem. Mater.*, 1999, **11**, 2310–2312.
27 I. Tanahashi and H. Kanno, *Appl. Phys. Lett.*, 2000, **77**, 3358–3360.
28 A. W. Adamson, W. L. Waltz, E. Zinato, D. W. Watts, P. D. Fleischauer and R. D. Lindholm, *Chem. Rev.*, 1968, **68**, 541–585.
29 S. Porel, S. Singh and T. P. Radhakrishnan, *Chem. Commun.*, 2005, 2387–2389.
30 T. Sato, T. Ito, H. Iwabuchi and Y. Yonezawa, *J. Mater. Chem.*, 1997, **7**, 1837–1840.
31 K. Esumi, T. Matsumoto, Y. Seto and T. Yoshimura, *J. Colloid Interface Sci.*, 2005, **284**, 199–203.
32 T. Itakura, K. Torigoe and K. Esumi, *Langmuir*, 1995, **11**, 4129–4134.
33 H. Hada, Y. Yonezawa, A. Yoshida and A. Kurakake, *J. Phys. Chem.*, 1976, **80**, 2728–2731.
34 R. M. Silverstein, G. C. Bassler and T. C. Morrill, *Spectrometric Identification of Organic Compounds*, John Wiley and Sons, New York, 5th edn., 1991.
35 C. W. Bunn, *Nature*, 1948, **161**, 929–930.
36 D. V. Leff, L. Brandt and J. R. Health, *Langmuir*, 1996, **12**, 4723–4730.
37 H. P. Klug and L. E. Alexander, *X-ray Diffraction Procedures: for Polycrystalline and Amorphous Materials*, Wiley, New York, 2nd edn., 1974.

